SAR PSEUDO DIFFERENCIAL INTERFEROGRAM MODELING

Prof. Andon Lazarov, Assist. Prof. Dimitar Minchev, Burgas Free University

***Abstract**: This work addresses an algorithm of Synthetic Aperture Radar (SAR) interferogram modeling to evaluate surface displacement. The interferogram obtained is called pseudo differential interferogram. Measurements of two SAR satellites placed in one and the same point of observation are used. Linear frequency modulated emitted signal is used to produce reflected by the surface SAR signal. Two-dimensional Fourier transform is applied to extract two single look complex (SLC) images. Pseudo differential interferogram showing the ground displacement is computed. To verify proposed model a numerical experiment realization implemented in MATLAB® environment is presented.*

***Key words**: InSAR, DInSAR, Differential SAR, Interferogram modeling.*

1. Introduction

Space based microwave instruments like Synthetic Aperture Radar (SAR), are advanced tools for monitoring the Earth's surface [1-7]. They are built on the principle of probing the earth's surface and objects on it with high informative electromagnetic pulses and registration of backscattered radiation from them. The resulting images are depicted in two-coordinates: slant range or time delay and azimuth or cross range. High resolution on the first coordinate is realized by using of bandwidth emitted pulses and on the second coordinate by coherent summation of reflected signals during the process of observation A particular application of SAR systems is in the field of SAR interferometry to extract three-dimensional images of observed objects, which uses amplitude and phase information of complex images of observed surface obtained by SAR systems [8-11]. One of the perspective methods of studying complex SAR images and their application in SAR interferometry is the mathematical modeling of the ground surface relief. There are different interpretations of this problem. Simulation model of surface topography on the basis of fractal Braun movement is presented in [12]. For modeling the intensity of backscattering radiation from the ground surface cosine function is applied [13]. The main purpose of this work is to propose a model for pseudo differential interferogram computation and illustrate surface displacement recognition technique.

2. Surface construction and displacement effect applying

The surface under observation is depicted in a Cartesian coordinate system *Oxyz* and analytically can be presented as a two dimensional surface function, i.e. the coordinate *z* as a function of coordinates *x* and *y*, which in discrete form is given by the following equation

$$\begin{aligned} z_{mn} = z_{mn}(x_{mn}, y_{mn}) &= 3(1-x_{mn})^2 \exp\left[-(x_{mn})^2 - (y_{mn}+1)^2\right] \\ &-10\left(\frac{x_{mn}}{5} - {x_{mn}}^3 - {y_{mn}}^5\right)\exp\left[{x_{mn}}^2 - {y_{mn}}^2\right] \\ &-\frac{1}{3}\exp\left[-(x_{mn}+1)^2 - {y_{mn}}^2\right] \end{aligned} \quad (1)$$

The equation (1) is implemented by modified MATLAB® function “peaks” by removing negative values, the result can be seen in the Fig.1, *a*. Modeling of surface

displacement is produced by reducing the height of a particular region and implemented by following programing code

$Surface_1 = (Z_{mn} > 0)$
$surface\_middle = max(max(Surface_1)) / 2;$
$index = (Surface_1 > surface\_middle);$
$elevation = (index .* Surface_1) ./ 1.2;$
$Surface_2 = Surface_1 - elevation + ((index .* surface\_middle)/1.2);$

As a result the original observed surface (Fig.1, *a*) is modified to new surface (Fig.1, *b*) in order to investigate displacement of the ground area. As can be seen the regions higher than 4.5 are removed from the second surface. This reduces almost two times the observed heights of the region of interest.

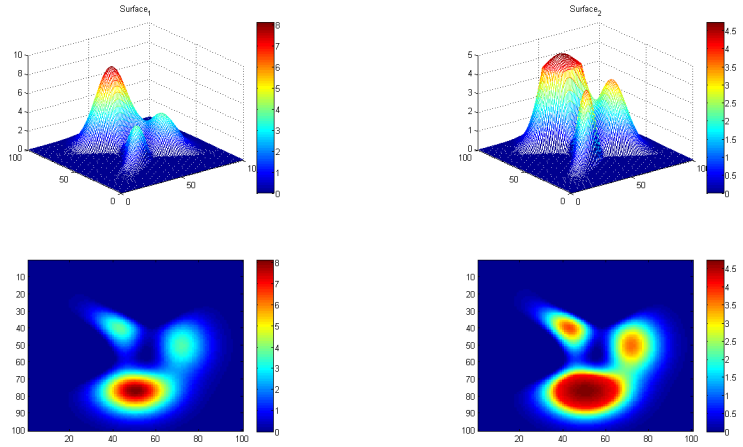

(*a*) (*b*)

Fig.1. Original surface (*a*); Modified surface (*b*);

3. SAR geometric description

The geometry information of the observed surface is contained in the phase of the complex amplitude of the reflected signal from each point scatterer which is proportional to the module of the distance vector $R_{mn}(p)$ defined by the expression

$$R_{mn}(p) = \sqrt{[x(p) - x_{mn}]^2 + [y(p) - y_{mn}]^2 + [z(p) - z_{mn}]^2} \quad (2)$$

SAR emits series of linear frequency modulated electromagnetic pulses which analytically can be described as

$$S(t) = \sum_{p=1}^{M} A \exp\left\{-j\left[\omega(t - pT_p) + b(t - pT_p)^2\right]\right\} \quad (3)$$

where A is the amplitude of the emitted pulse, T_p is the pulse repetition period, $\omega = 2\pi\frac{c}{\lambda}$ is the angular frequency, $p = \overline{1,\ N}$ is the current number of emitted LFM pulses, N is the number of emitted pulses during aperture synthesis, c = 3.10^8 m/s is the speed of the light, ΔF is the bandwidth of the emitted pulse, and defines the value of the range resolution element, i.e. $\Delta R = c/2\Delta F$, $b = \frac{\pi\Delta F}{T_k}$ is the LFM index, T_k is the time duration of LFM pulse.

The deterministic component of the SAR signal reflected from the *mn*-th point scatterer is a finite function and can be written as

$$S_{mn}(t) = \mathbf{rect}\frac{t - t_{mn}}{T_k}.\exp\left\{-j\left[\omega(t - t_{mn}) + b(t - t_{mn})^2\right]\right\} \quad (4)$$

where

$$\mathbf{rect}\frac{t - t_{mn}(p)}{T_k} = \begin{cases} 0, \frac{t - t_{mn}(p)}{T_k} \le 0 \\ 1, \frac{t - t_{mn}(p)}{T_k} \le 1 \\ 0, \frac{t - t_{mn}(p)}{T_k} > 1 \end{cases}, \quad (5)$$

is the rectangular function; $t_{mn}(p) = \frac{2R_{mn}(p)}{c}$ is the time delay of the signal from the *mn*-th point scatterer.

The deterministic component of the SAR signal reflected from the entire surface can be regarded as a geometrical sum of the signals reflected by all point scatterers signals from the surface of observation and can be expressed as

$$S(t) = \sum_n \sum_m \mathbf{rect}\frac{t - t_{mn}(p)}{T_k}.\exp\left\{-j\left[\omega(t - t_{mn}(p)) + b(t - t_{mn}(p))^2\right]\right\} \quad (6)$$

The time dwell t in discrete form for each signal return for each emitted pulse p is defined by (7):

$$t = t_{mn\min}(p) + (k-1)\Delta T\ , \quad (7)$$

where $k = \overline{1, K_{\max}(p)}$ is the index of the time discrete, $\Delta T = 1/2\Delta F$ is the time duration of the LFM sample, ΔF is the bandwidth of the emitted LFM pulse, $K_{\max}(p)$ is the number of the range bin where the SAR signal from the furthest point scatterer is detected, $t_{mn\min}(p) = \frac{2R_{mn\min}(p)}{c}$ is the time delay of the signal from the nearest point scatteter, $R_{mn\min}(p)$ - is the distance to the nearest point scatteter from the surface of observation for the p-th emitted pulse.

The substitution of the equation (7) in the expression (6) yields the following computational equation in discrete form

$$\dot{S}(p,k) = \sum_n \sum_m \mathbf{rect} \frac{t_{mn\min}(p) + (k-1)\Delta T - t_{mn}(p)}{T_k} \times \tag{8}$$
$$\times \exp\left\{ -j \left[\begin{array}{l} \omega\left(t_{mn\min}(p) + (k-1)\Delta T - t_{mn}(p)\right) + \\ + b\left(t_{mn\min}(p) + (k-1)\Delta T - t_{mn}(p)\right)^2 \end{array} \right] \right\}.$$

The expressions (2-8) can be used to modeling of SAR signals reflected from the surface with complicated relief, as example Fig.1.

4. SAR image reconstruction algorithm

Consider the case of side looking SAR satellite system. The image of the surface will be extracted at the moment $p = N/2$ corresponding to the middle of the synthetic aperture. The number of emitted pulses N, the velocity of satellite and the pulse repetition period are chosen to guarantee variation of the phase of the reflected signal during aperture synthesis no more than $\pi/2$. Therefore additional phase correction and focusing procedures are not required. It allows image reconstruction to be reduced to two dimensional Fourier transforms to the demodulated complex SAR signal, i.e.

$$\dot{S}(\bar{k},\bar{p}) = \sum_{p=1}^{N} \left[\sum_{k=1}^{K} \tilde{S}(k,p) \exp\left(-j \frac{2\pi k \bar{k}}{K+L} \right) \right] \exp\left(-j \frac{2\pi p \bar{p}}{N} \right) \tag{9}$$

which can be implemented by the procedure of Fast Fourier Transform (FFT) in MATLAB®

$$\dot{S}(\bar{k},\bar{p}) = \mathrm{FFT}_p[\mathrm{FFT}_k(\tilde{S}(k,p)] \tag{10}$$

where $\tilde{S}(k,p) = S(k,p)\exp\left\{ j\omega(k-1)\Delta T + b((k-1)\Delta T)^2 \right\}$ is the demodulated SAR signal, $\dot{S}(\bar{k},\bar{p})$ is the complex image containing amplitude and phase information of the image of the observed surface.

The SAR image reconstruction algorithm presented by (9) and (10) is used for generating two single look complex images, master and slave shown in Fig.2. The master and slave image produce pseudo differential interferogram by mutual complex conjugate multiplication after coregistration.

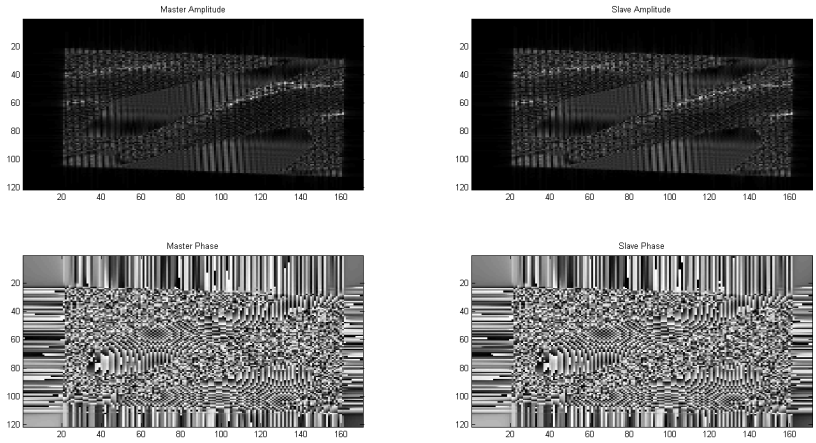

(*a*) (*b*)

Fig.2. Master image amplitude and phase (*a*), Slave image amplitude and phase (*b*)

5. Coherence map and interferogram computation

The master complex image can be analytically defined by the expression

$$\begin{aligned} \dot{A}_M &= A_M.e^{i\Phi_M} = \mathrm{Re}(\dot{A}_M) + j\,\mathrm{Im}(\dot{A}_M) \\ A_M &= \sqrt{\mathrm{Re}^2(\dot{A}_M) + \mathrm{Im}^2(\dot{A}_M)} \\ \Phi_M &= arctg\left(\frac{\mathrm{Im}(\dot{A}_M)}{\mathrm{Re}(\dot{A}_M)}\right) \end{aligned} \qquad (11)$$

where A_M is the amplitude and Φ_M is the phase of the master complex image.
The slave complex image can be analytically defined by the expression

$$\begin{aligned} \dot{A}_S &= A_S.e^{i\Phi_S} = \mathrm{Re}(\dot{A}_S) + j\,\mathrm{Im}(\dot{A}_S) \\ A_S &= \sqrt{\mathrm{Re}^2(\dot{A}_S) + \mathrm{Im}^2(\dot{A}_S)} \\ \Phi_S &= arctg\left(\frac{\mathrm{Im}(\dot{A}_S)}{\mathrm{Re}(\dot{A}_S)}\right) \end{aligned} \qquad (12)$$

where A_S is the amplitude and Φ_S is the phase of the slave complex image.
The complex interferogram (*pseudo differential interferogram*) can be calculated by complex conjugate of the master and slave complex images, expressed by equation

$$\dot{I} = \dot{A}_M * \dot{A}_S^* = A_M.e^{i\Phi_M} A_S.e^{-i\Phi_S} = A_M A_S.e^{i(\Phi_M - \Phi_S)} \qquad (13)$$

The modulus of the complex interferogram (13) is the coherence map, while the phase is the actual interferogram, as can be seen in equation

$$
\begin{aligned}
Coh &= A_M A_S = \sqrt{\mathrm{Re}^2(\dot{I}) + \mathrm{Im}^2(\dot{I})} \\
Int &= arctg\left(\frac{\mathrm{Im}(\dot{I})}{\mathrm{Re}(\dot{I})}\right)
\end{aligned} \tag{14}
$$

In MATLAB® environment, *Coh* can be obtained by function ABS, and *Int* can be obtained by function ANGLE. The experimental results are illustrated in Fig.3. In Fig.3b the deformation caused by surface modification is represented. In the interferogram (Fig.3b) can be seen the area from the surfaces that have been artificially distorted.

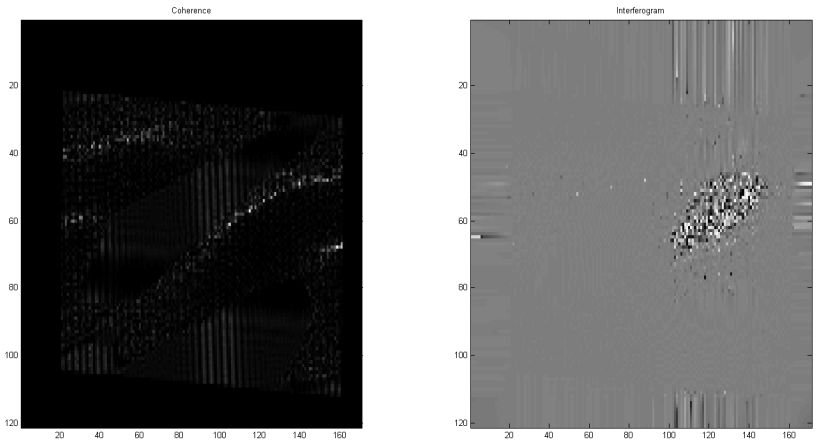

(*a*) (*b*)

Fig.3 Coherence map (*a*), Interferogram (*b*).

6. Conclusion

In this work an algorithm for generation of SAR pseudo differential interferogram to evaluate surface displacement has been suggested. A SAR emitted signal with linear frequency modulation has been used to produce the model of a SAR signal reflected by the surface. All stages of SAR signal modeling including surface geometry signal formation and image reconstruction process are described. Two-dimensional Fourier transform have been applied to obtain two single look complex images acquired from one and the same position of the satellites. The algorithm of pseudo differential interferogram has been suggested. The analysis of pseudo differential interferogram shows the ground displacement. To verify proposed geometrical and signal models and image reconstruction algorithms a numerical experiment implemented in MATLAB® environment have been presented.

Acknowledgment
This work is supported by NATO CLG: ESP.EAP.CLG.983876

References

1. R. Bamler “A Comparison of Range-Doppler and Wavenumber Domain SAR Focusing Algorithms”, IEEE Trans. on GRS, 1992, 30(4): 706-713.

2. R. K. Raney, “Precision SAR Processing Using Chirp Scaling”, IEEE Trans. on GRS, 1994, 32(4): 786-799.
3. R. K. Raney, “An exact wide field digital imaging algorithm”, International Journal of Remote Sensing, 1992, 13(5): 991-998.
4. A. Moreira, “Airborne SAR Processing of Highly Squinted Data Using a Chirp Scaling Algorithm with Motion Compensation”, IEEE Trans. on GRS, 1994, 32(5): 1029-1040.
5. Bryant, M., L. Bryant, L. Gostin, M. Soumekh. 3-D E-CSAR Imaging of a T-72 Tank and Synthesis of its SAR Reconstructions. IEEE Trans. on AES, vol. 39, No. 1 January, 2003.
6. Jeong, H., J. H. Park, J. B. Kwon, Y. Oh,VLSI Architecture for SAR Data, Com press ion, IEEE Trans. on AES vol: 38, No. 2 April, 2002
7. Neo, Y.L., Fr. Wong, and Ian G Cumming. A two-dimensional spectrum for bistatic SAR processing using series reversion. *Geoscience and Remote Sensing Letters*, 4(1):93-97, January 2007.
8. Nicolas, J-M, G. Vasile, M. Gay, Fl. Tupin, and Em. Trouvé. SAR processing in the temporal domain: application to direct interferogram generation and mountain glacier monitoring *Can. J. Remote Sensing*, Vol. 33, No. 1, pp. 52–59, 2007.
9. Van Leijen, F. R. Hanssen. Interferometric radar meteorology: resolving the acquisition ambiguity. In *CEOS SAR Workshop, Ulm Germany, 27-28 May 2004*, page 6, 2004.
10. Colesanti, C., Al. Ferretti, F. Novali, Cl. Prati, and F. Rocca. SAR monitoring of progressive and seasonal ground deformation using the Permanent Scatterers Technique. *IEEE Transactions on Geoscience and Remote Sensing*, 41(7): 1685-1701, July 2003.
11. Pi, Y., H. Long, Sh. Huang. A SAR parallel processing algorithm and its implementation, Pecora 15/Land Satellite Information IV/ISPRS Commission I/FIEOS 2002 Conference Proceedings.
12. Julea, A., G. Vasile, Iv. Petilot, Em.Trouve, M. Gay, J-M. Nicolas, Ph. Bolon, Simulation of SAR Images and Radar Coding of Georeferenced Information for Temperate Glacier Monitoring, Laboratoire d'Informatique, Systμemes, Traitement de l'Information et de la Connaissance, Universite de Savoie - ESIA - BP 806 - F-74016 Annecy Cedex – FRANCE.
13. K. Ren, G. Wu, X.Q.Shi, and V. Prinet. Simulation of interferograms for spaceborn SAR system**,** Dept. of Electronic Engineering, Nanjing University of Sciences and Technology, Nanjing, National Laboratory of Pattern Recognition, Institute of Automation, CAS.